THE JOURNAL OF PHYSICAL CHEMISTRY B

Article

pubs.acs.org/JPCB

Terms of Use

Interfacial Bond-Breaking Electron Transfer in Mixed Water−Ethylene Glycol Solutions: Reorganization Energy and Interplay between Different Solvent Modes

Oksana Ismailova,[†] Alexander S. Berezin,[‡] Michael Probst,*[,§] and Renat R. Nazmutdinov*[,‡]

[†]Institute of Ion-Plasma and Laser Technology, Academy of Sciences of Uzbekistan, 100125 Tashkent, Uzbekistan

[‡]Kazan National Research Technological University, 420015 Kazan, Republic of Tatarstan, Russian Federation

[§]Institute of Ion Physics and Applied Physics, University of Innsbruck, 6020 Innsbruck, Austria

Supporting Information

ABSTRACT: We explore solvent dynamics effects in interfacial bond breaking electron transfer in terms of a multimode approach and make an attempt to interpret challenging recent experimental results (the nonmonotonous behavior of the rate constant of electroreduction of $S_2O_8^{2-}$ from mixed water−EG solutions when increasing the EG fraction; see Zagrebin, P.A. et al. *J. Phys. Chem. B* **2010**, *114*, 311). The exact expansion of the solvent correlation function (calculated using experimental dielectric spectra) in a series predicts the splitting of solvent coordinate in three independent modes characterized by different relaxation times. This makes it possible to construct a 5D free-energy surface along three solvent coordinates and one intramolecular degree of freedom describing first electron transfer at the reduction of a peroxodisulphate anion. Classical molecular dynamics simulations were performed to study the solvation of a peroxodisulphate anion ($S_2O_8^{2-}$) in oxidized and reduced states in pure water and ethylene glycol (EG) as well as mixed H_2O−EG solutions. The solvent reorganization energy of the first electron-transfer step at the reduction of $S_2O_8^{2-}$ was calculated for several compositions of the mixed solution. This quantity was found to be significantly asymmetric. (The reorganization energies of reduction and oxidation differ from each other.) The averaged reorganization energy slightly increases with increasing the EG content in solution. This finding clearly indicates that for the reaction under study the static solvent effect no longer competes with solvent dynamics. Brownian dynamics simulations were performed to calculate the electron-transfer rate constants as a function of the solvent composition. The results of the simulations explain the experimental data, at least qualitatively.

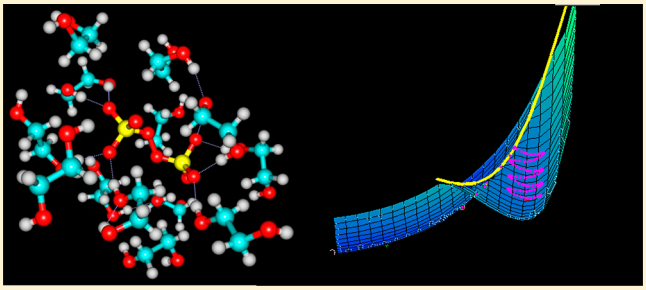

1. INTRODUCTION

The electrochemical reduction of a peroxodisulphate anion ($S_2O_8^{2-}$) is a well-known reaction, although some details of its mechanism are not properly understood so far. This is a good example of bond-breaking electron transfer; the reaction takes place in the vicinity of activationless discharge and demonstrates a "polarization pit" on the current−voltage curves as well as cation catalysis (see works[1,2] and refs therein). Such qualitatively interesting features of this electrochemical redox process make it attractive to employ modern quantum mechanical theory of charge transfer in condensed media.[3,4] This has been done in works[1,2] with the help of quantum chemical modeling. The reduction of $S_2O_8^{2-}$ on a mercury electrode from solutions with variable viscosity (water−sugar and water−ethylene glycol (EG) mixtures) was investigated experimentally as well.[5,6] The current−solution viscosity dependences built for overvoltage values in the region of the "polarization pit" reveal a challenging nonmonotonous behavior: the current decreases first reaching a plateau. However, it begins to increase from a certain viscosity value.[6] As the reduction of $S_2O_8^{2-}$ is accompanied by the −O−O− bond break, the intramolecular reorganization plays a crucial role. Another important driving force of this electron-transfer process is solvent (outer sphere, or environmental) reorganization. One needs, therefore, at least a 3D reaction free-energy surface (along solvent and intramolecular coordinates) to calculate the activation barrier. The experimental data obtained for water−sugar mixtures[5] were interpreted in ref 7 by considering the interplay between two effects of different nature: the first one originates from a pure solvent dynamics (i.e., slow diffusion along the solvent coordinate) and leads to a decrease in the rate constant when the solvent viscosity increases. In contrast, the second effect is solely of static nature and results from the decrease in solvent reorganization energy with increasing viscosity due to the change of dielectric properties of mixed solutions.

Received: January 16, 2013
Revised: June 16, 2013
Published: June 17, 2013

 © 2013 American Chemical Society dx.doi.org/10.1021/jp405097c | *J. Phys. Chem. B* 2013, 117, 8793−8801

The "static" effect was demonstrated to play a crucial role in describing the experimentally observable effects[7] on the basis of the Sumi−Marcus model,[8] where only one solvent mode is addressed. Therefore, it would be tempting to extend such an approach to elucidate the results obtained in ref 6 for water−EG mixtures as well. It was formerly assumed[6] on the basis of an analysis of the solvent correlation function that the experimental effect might result from the interplay of dynamical properties of different solvent modes. The main aim of this work is to check this hypothesis performing Brownian dynamics simulations.

A preliminary analysis of the Pekar factor ($C = 1/\varepsilon_\infty - 1/\varepsilon_0$, where ε_∞ and ε_0 are the optical (fast) and static (slow) medium dielectric constants, respectively) versus EG content in mixed solutions points to a very slight static effect.[6] Because solvent reorganization energy is an important parameter in the above-mentioned calculations, it is therefore worth it to go beyond simplified continuum approaches and to describe a possible "static" solvent effect in water−EG solutions at the reduction of $S_2O_8^{2-}$ at atomistic level. The dependence of solvent reorganization on the composition of various mixed solvents in the regime of homogeneous ET mixed solvents was thoroughly investigated for a number of redox couples in works.[9−13] This quantity was extracted from experimental rate constants as well as estimated using model calculations. The authors put primary attention on the analysis of the Pekar factor as a function of the solution composition (this dependence can be both linear and nonlinear) and concluded that preferential solvation crucially affects the solvent reorganization.

The paper is organized as follows: In Section 2, pertinent model and computational details are reported. The solvation energies of $S_2O_8^{2-}$, the structure of nearest solvation shell of reactant, and the reorganization energies are discussed in Section 3. The model rate constants calculated for different water−EG mixtures are presented in this Section as well. Some concluding remarks can be found in Section 4.

2. COMPUTATIONAL DETAILS

Solvent Correlation Function and Brownian Dynamics. In our work a correlation function $M(\tau) = \langle \varepsilon_A(\tau)\varepsilon_A(0)\rangle$ describing the fluctuating reactant energy level in solution $\varepsilon_A(\tau)$ plays an important role. This function can be calculated directly from molecular dynamics simulations. However, following a more general and flexible way we will employ another formalism:[14]

$$M(\tau) = 2k_B T\lambda_s \frac{Q(\tau)}{Q(0)} \tag{1}$$

where λ_s is solvent reorganization energy and $Q(\tau)$ is a function of the complex dielectric spectrum $\varepsilon(\omega)$:

$$Q(\tau) = \frac{i}{2\pi}\int_{-\infty}^{\infty} \exp(-i\omega\tau)\left[\frac{1}{\varepsilon(\omega)} - \frac{1}{\varepsilon_0}\right]\frac{d\omega}{\omega} \tag{2}$$

with ε_0 being the static dielectric constant, $\varepsilon_0 = \varepsilon(\omega \to 0)$. (The frequency-dependent function $1/\varepsilon(\omega) - 1/\varepsilon_0$ can be treated as a generalized Pekar factor.)

For the $S_2O_8^{2-}$ reduction the solvent reorganization energy in eq 1 refers to the bond-breaking first electron transfer:

$$S_2O_8^{2-} + e = S_2O_8^{3-} = SO_4^{2-} + SO_4^{-} \tag{3}$$

This step is rate-controlling; the second step (reduction of the SO_4^- radical) proceeds significantly faster. It was found in work[6] that the dielectric spectrum for water−EG mixtures reveals a 3-D behavior:

$$\varepsilon(\omega) = \frac{\Delta\varepsilon_1}{1 + i\omega\tau_1} + \frac{\Delta\varepsilon_2}{1 + i\omega\tau_2} + \frac{\Delta\varepsilon_3}{1 + i\omega\tau_3} + \varepsilon_\infty \tag{4}$$

where τ_i are characteristic relaxation times.

For such solvents the correlation function $M(\tau)$ can be exactly expanded into the sum:[15,16]

$$M(\tau) = 2k_B T\lambda_s \sum_{i=1}^{3} \delta_i \exp(-\tau/\tau_i^*) \tag{5}$$

where the δ_i are contributions to the solvent reorganization energy λ_s from ith solvent mode ($\sum_{i=1}^{3}\delta_i = 1$) and τ_i^* are their relaxation times.

To perform the expansion of $M(\tau)$, we used the data on the water −EG dielectric spectra reported in ref 6 and employed an inverse Laplace transform technique using the *Mathematica 8* program suite. The results are shown in Figure 1 and reveal a different behavior of the different solvent modes. The lowest relaxation time contributes slightly to the solvent reorganization energy; however, its effect becomes more noticeable at higher EG content. The contribution of the fast mode decreases with the EG content, while the middle mode changes opposite. The most important consequence of expansion 5 is that we can introduce three independent solvent coordinates $\vec{q} = (q_1, q_2, q_3)$ to address the solvent contribution to the multidimensional

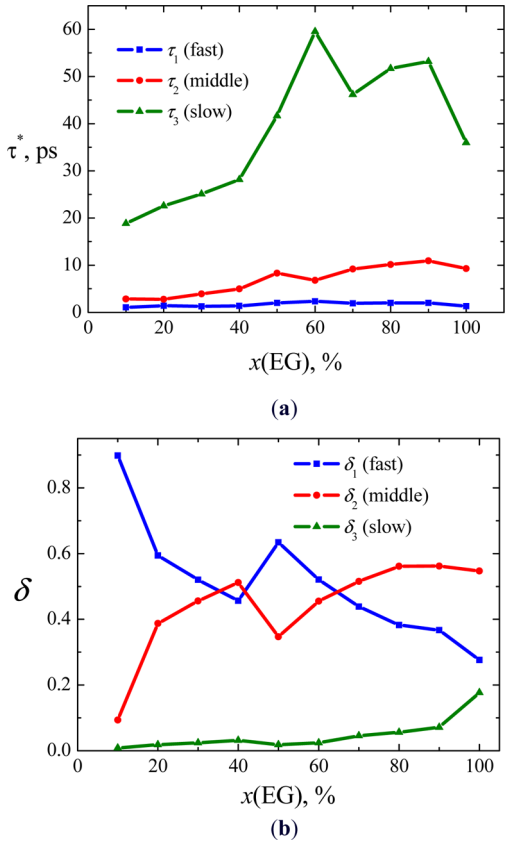

Figure 1. Three solvent relaxation times τ_i^* (a) and their contributions to the reorganization energy δ_i. (b) Calculated for EG-water mixtures using experimental dielectric spectra (see eq 5).

dx.doi.org/10.1021/jp405097c | J. Phys. Chem. B 2013, 117, 8793−8801

reaction free-energy surface E_i. In the weak coupling limit (small reactant−electrode orbital overlap) this surface can be recast in the form:

$$E_i(\vec{q}, r) = U_i(\vec{q}) + U_i^*(r) \quad (6)$$

and

$$E_f(\vec{q}, r) = U_f(\vec{q}) + U_f^*(r) - e_0\eta \quad (7)$$

where r is the intramolecular coordinate (the O−O bond length in peroxodisulfate); indices i and f refer to the initial and final states, respectively; η is electrode overvoltage. The "solvent" parts of eqs 6 and 7, $U_i(\vec{q})$ and $U_f(\vec{q})$, take the form:

$$U_i(\vec{q}) = \sum_{j=1}^{3} \delta_j \lambda_s q_j^2 \quad (8)$$

and

$$U_i(\vec{q}) = \sum_{j=1}^{3} \delta_j \lambda_s (q_j - 1)^2 \quad (9)$$

The potentials describing the intramolecular reorganization of a peroxodisulphate anion were obtained from DFT calculations in ref 1:

$$U_i^*(r) = D(1 - \exp[-\alpha r])^2 \text{ and } U_f^*(r) = B \exp[-\beta r] \quad (10)$$

where D = 1.86 eV; α = 2.38 Å^{-1}; B = 3.709 eV; and β = 1.95 Å^{-1}.

A theoretical analysis of the outer-sphere electron transfer in solvents with two characteristic relaxation times was performed by the authors in ref 17. They used the Agmond−Hopfield formalism[8] to make numerical estimations of the rate constant. Because we have to deal with a partial differential equation, a similar analysis is hardly possible in our case. (See pertinent discussion in ref 6.) Therefore, we employed Langevin (Brownian) molecular dynamics[18] to calculate the reaction rate (k). A system of four differential equations describes the motion in a 5D reaction space along three solvent coordinates and one intramolecular degree of freedom:

$$\begin{aligned}
\frac{\partial q_1}{\partial \tau} &= -\frac{1}{2\delta_1\lambda_s\tau_1^*}\frac{\partial U_i}{\partial q_1} + \frac{dq_1^{rand}}{d\tau} \\
\frac{\partial q_2}{\partial \tau} &= -\frac{1}{2\delta_2\lambda_s\tau_2^*}\frac{\partial U_i}{\partial q_2} + \frac{dq_2^{rand}}{d\tau} \\
\frac{\partial q_3}{\partial \tau} &= -\frac{1}{2\delta_3\lambda_s\tau_3^*}\frac{\partial U_i}{\partial q_3} + \frac{dq_3^{rand}}{d\tau} \\
\frac{\partial^2 r}{\partial \tau^2} &= -\frac{1}{m}\frac{\partial U_i^*}{\partial r} - \gamma_r\frac{dr}{d\tau} + \frac{dv^{rand}}{d\tau}
\end{aligned} \quad (11)$$

where m is the reduced mass of $S_2O_8^{2-}$; dq_1^{rand}, dq_2^{rand}, dq_3^{rand} are random increments of solvent coordinates; dv^{rand} is a random increment of velocity for the movement along the r coordinate; and γ_r is the intramolecular friction coefficient.

In eq 11, the first three equations describe the solvent dynamics in an overdamped regime;[4] the solvent coordinates are treated as slow. In opposite, the intramolecular coordinate was found to be fast. The random increments were generated according to the algorithm presented in ref 18. This algorithm presumes constructing Gaussian-like distribution functions for the random increments (see eq 11), which depend on friction coefficients γ_i. The latter were defined in the following way:[4]

$$\gamma_i = \tau_i^* \omega_i^2 \quad (12)$$

The frequencies ω_i in eq 12 were estimated from the system of equations:[3]

$$\begin{aligned}
\omega_{eff}^2 &= \delta_1\omega_1^2 + \delta_2\omega_2^2 + \delta_3\omega_3^2, \\
(\omega_1/\omega_2)^2 &= \delta_1/\delta_2, \\
(\omega_1/\omega_3)^2 &= \delta_1/\delta_3
\end{aligned} \quad (13)$$

where $\omega_{eff} = 10^{13}$ Hz.

To estimate the intramolecular friction coefficient γ_r, we took a value of 1 ps for the relaxation time;[7] the corresponding frequency was calculated for the bottom of the Morse potential $U_i^*(r)$. A set of the reactant life times ($\tau_{life,i}$) was computed by generating several thousands trajectories. The lifetime for the ith trajectory is defined as time that is required to reach the reaction saddle line starting from the bottom of initial well. The resulting lifetime is their average:

$$<\tau_{life}> = \frac{1}{N}\sum_{i=1}^{N} \tau_{life,i} \quad (14)$$

where N is the number of trajectories (in our simulations N = 12 000).

Then, the rate constant k can be estimated as $1/<\tau_{life}>$. The system was integrated by the Verlet method with the help of a *Matlab 2009b* program with an integration step of 1 ps. The reliability of the computational scheme (eqs 11) was tested first for a simple two-well potential

A crucial point for further estimations of the rate constant is a possible dependence of the solvent reorganization energy on the solution viscosity (EG content), that is, "static" solvent effect (see Introduction). To elucidate this issue, we have performed atomistic molecular dynamics simulations for $S_2O_8^{2-/3-}$ in water−EG mixed solvents. Some details are reported in the next section.

Solvent Reorganization Energy. In general, the solvent reorganization energy should be calculated in the vicinity of the activation barrier, that is, for an elongated O−O bond length. For the sake of simplicity, however, all molecular dynamics simulations were performed for the geometry of the optimized oxidized state, $S_2O_8^{2-}$ (independent of the total charge of reactant, −2 or −3).

The frequently used way to calculate the solvent reorganization energy from molecular dynamics simulations is based on the following equation for the reaction free-energy surface $G_{i(f)}$ as function of a collective solvent coordinate ΔE (see, for example, ref 19)

$$G_{i(f)}(\Delta E) = -k_B T \ln\{f(\Delta E)\} \quad (15)$$

where ΔE is the energy of Coulomb interaction of a reactant or product with solvent molecules; f is a distribution function that shows a probability to reach a certain ΔE interval due to statistical fluctuations of solvent molecules; and indexes i and f refer to reactant and product, respectively.

After $G_i(\Delta E)$ and $G_f(\Delta E)$ are built, one can fit both curves (assuming a linear response from the solvent environment) by intersecting parabolas and estimate both the activation barrier and the reorganization energies of reduction ($\vec{\lambda}_s$) and oxidation

dx.doi.org/10.1021/jp405097c | J. Phys. Chem. B 2013, 117, 8793−8801

($\overleftarrow{\lambda}_s$) as a difference between nonequilibrium and equilibrium solvation energies of reactant and product, respectively. Some results of such calculations obtained for $x(EG) = 0.5$ are presented as an illustration in the Supporting Information (see Figure 1S, Section A2). This approach is, however, rather computer time demanding, as its accuracy noticeably depends on the ensemble size and simulation time. A special bias sampling technique is employed as well to perform more efficient calculations.[19] In this work we use a more simplified method to estimate $\vec{\lambda}_s$ and $\overleftarrow{\lambda}_s$:

$$\vec{\lambda}_s = E_{noneq}(S_2O_8^{2-}) - E_{eq}(S_2O_8^{2-}) \quad (16)$$

where $E_{eq}(S_2O_8^{2-})$ is the interaction energy of $S_2O_8^{2-}$ with solvent molecules in configurations, which are in equilibrium for $S_2O_8^{2-}$; $E_{noneq}(S_2O_8^{2-})$ is the interaction energy of $S_2O_8^{2-}$ with solvent molecules in configurations that are equilibrium for $S_2O_8^{3-}$. In turn

$$\overleftarrow{\lambda}_s = E_{noneq}(S_2O_8^{3-}) - E_{eq}(S_2O_8^{3-}) \quad (17)$$

where $E_{eq}(S_2O_8^{3-})$ is the interaction energy of $S_2O_8^{3-}$ with solvent molecules in configurations that are in equilibrium for $S_2O_8^{3-}$ and $E_{noneq}(S_2O_8^{3-})$ is the interaction energy of $S_2O_8^{3-}$ with solvent molecules in configurations which are in equilibrium for $S_2O_8^{2-}$.

Of course, the linear response theory (LRT) is sometimes too crude to describe solvent contribution to the activation barrier of electron transfer in a proper way. Deviations from the LRT were thoroughly analyzed in work;[20] a new three-parametric model was developed as well.[20] The behavior of the transfer coefficient in interfacial electron transfer reactions was theoretically investigated in ref 21, assuming a nonlinear solvent response. Redox reactions at the interface of an active protein to water might be another example of systems, where nonlinear effects (nongauss fluctuations of solvent molecules) take place.[22] Nevertheless, the solvent reorganization energy still remains a convenient and commonly adopted language to describe the Franck−Condon barrier in homogeneous electron-transfer reactions in mixed solvents.[9−13] It is important to note that in this work we are interested first of all in addressing the qualitative behavior of the solvent reorganization energy as a function of the EG content in solutions; this justifies to some extent the simplified approach used to estimate the λ_s values (eqs 16, 17).

Potential Energy Functions and Details of the Simulations. The geometry of peroxodisulfate ion with charge $q = -2$ was optimized by the Möller−Plesset many-body perturbation theory (MP2) using the standard 6-31++G(d, p) basis set. Atomic partial charges in the $S_2O_8^{2-}$ and $S_2O_8^{3-}$ ions were computed with the restrained electrostatic potential (RESP) model.[23] All interactions are described with Lennard-Jones pair potentials and atomic partial charges:

$$V_{ij}(r_{ij}) = V_{ij}^{el}(r_{ij}) + V_{ij}^{LJ}(r_{ij}) = \frac{q_i q_j}{r_{ij}} + 4\varepsilon_{ij}\left[\left(\frac{\sigma_{ij}}{r_{ij}}\right)^{12} - \left(\frac{\sigma_{ij}}{r_{ij}}\right)^{6}\right] \quad (18)$$

where q_i and q_j are the partial charges of atoms i and j; r_{ij} is the distance between these atoms; σ is the van der Waals diameter, $\sigma_{ij} = 1/2(\sigma_i + \sigma_i)$; and ε is the depth of the potential well, $\varepsilon_{ij} = (\varepsilon_i\varepsilon_j)^{1/2}$.

The interaction parameters and partial charges used in this work are listed in Table 1S (see Supporting Information, Section A1). The Amber force fields[24] were adapted to reproduce the solvation free energy of $S_2O_8^{2-}$ by slightly modifying the partial charges of oxygen and sulfur atoms and were employed for $S_2O_8^{2-}$ and $S_2O_8^{3-}$ interacting with water and EG. For water, we used the SPC/E model,[25] which describes fairly well the radial distribution function of the oxygen atoms, other structural parameters, and the water dielectric constant.[26] The SPC/E model is rigid with oxygen−hydrogen distances fixed at 1.0 Å and the valence angle at 109.47°. Partial charges of $-0.847q$ and $+0.423q$ reside on oxygen and hydrogen, respectively (q is the elementary charge). For the EG−EG interactions we used a model developed by Kusalik et al.,[27] where authors used the all-atom AMBER/OPLS force field[28] with MM3[29] torsions, as shown in Table IS in the Supporting Information.

Simulations on peroxodisulfate in liquid water were performed at constant pressure and temperature using the Berendsen algorithm for maintaining constant pressure and temperature in a cubic box (starting dimensions 25 × 25 × 25 Å^3) filled with 503 water molecules. The equations of motion were solved using the Verlet algorithm with a 1 fs time step. Long-range Coulomb forces were addressed by the Ewald method. All of the other interactions were calculated within a sphere with a radius of R_{cutoff} = 9 Å.

Calculations on pure EG were performed in a periodic cubic box (starting size 37.6 × 37.6 × 37.6 Å^3) filled with 570 EG molecules. Here we have used the Parrinello−Rahman algorithm with 10.5 Å cutoff for maintaining constant pressure and temperature; the C−H and O−H bonds were constrained using the LINCS algorithm. The value of the static dielectric constant is important to study reorganization energies of pure and binary solutions.[11] The model we employed gives a value of 37 for the dielectric constant of pure EG, which is close to experimental data.[30] The Gibbs energy of solvation of peroxodisulfate ion in EG/water mixtures was calculated by the thermodynamic integration method;[31] pertinent corrections[32−37] were addressed as well. Electrostatic and van der Waals contributions were integrated at 12 discrete steps along $0 \le \lambda \le 1$. The simulation time for each value of λ was 240 and 40 ps discarded for equilibration. All simulations were performed using the GROMACS 4.5.3 package of computer codes.[38]

3. RESULTS AND DISCUSSION

The solvation free energies ΔG_{solv} of $S_2O_8^{2-}$ calculated for four values of the EG mole fraction are collected in Table 1.

Table 1. Solvation Free Energy of Peroxodisufate in Pure Water and EG and in Mixed Solutions Calculated from MD Simulations[a]

x(EG)	0	0.3	0.5	1
$-\Delta G_{solv}$, kcal mol^{-1}	200 (176.4)	199	196.5	174.4 (174.2)

[a]Solvation free energies obtained from DFT calculations and the polarized continuum model (PCM)[50] are given in parentheses.

The solvation energy decreases from water to pure EG. Because there are no available experimental data on the solvation energies of a peroxodisulfate anion, additional estimates of ΔG_{solv} were obtained for pure water and EG from DFT calculations with the polarizable continuum model (PCM). For EG the agreement between this estimate and the

dx.doi.org/10.1021/jp405097c | J. Phys. Chem. B 2013, 117, 8793−8801

one obtained from MD simulations is surprisingly good, while for water the difference between two predictions is larger.

As can be seen from Figure 2, the shape of radial distribution functions calculated for $S_2O_8^{2-}$ and $S_2O_8^{3-}$ in water differ

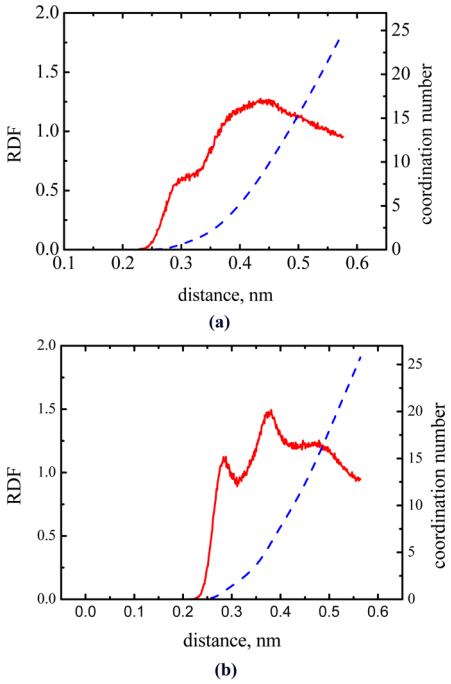

Figure 2. Coordination number (dashed line) plotted up to first minimum of the radial distribution function (solid line, left) calculated for $S_2O_8^{2-}$ (a) and $S_2O_8^{3-}$ (b) in water (x(EG) = 0).

noticeably from each other. The RDF for $S_2O_8^{3-}$ has a shoulder and a main peak, while for $S_2O_8^{3-}$ it reveals two peaks and a small plateau in the vicinity of the first RDF minimum. Similar features can be observed for the RDF with EG (Figure 3). Two smooth maxima on the RDF for the peroxodisulphate anion become sharper for its reduced form. The coordination numbers (n_{coord}) characterizing the nearest solvation sheath of the anion were found about two times smaller for EG as compared with water. (See Table 2.) These quantities change only slightly going from the oxidized to reduced state. For water, we observe an increase in n_{coord} by 1; in contrast, n_{coord} for EG decreases by 1.

The solvent reorganization energies are presented in Table 3. The environmental reorganization was found to be strongly asymmetric (the effect of the asymmetric intramolecular reorganization on the activation barrier of interfacial electron transfer reactions was thoroughly investigated in work[51]), that is, $\vec{\lambda}_s$ and $\overleftarrow{\lambda}_s$ values differ significantly; the asymmetry parameter $\nu = \vec{\lambda}_s/\overleftarrow{\lambda}_s$ ranges from 0.2 to 1.2. The average values (λ_s) were computed using the formula:[39,40]

$$\lambda_s = \frac{4\vec{\lambda}_s\overleftarrow{\lambda}_s}{(\sqrt{\vec{\lambda}_s} + \sqrt{\overleftarrow{\lambda}_s})^2} \tag{19}$$

It can be seen from Table 3 that the averaged reorganization energy increases slightly and nonmonotonously with increasing EG content. In other words, the activation barrier of electron transfer does not decrease with the growth of the solution viscosity and can be treated nearly constant. This is the most

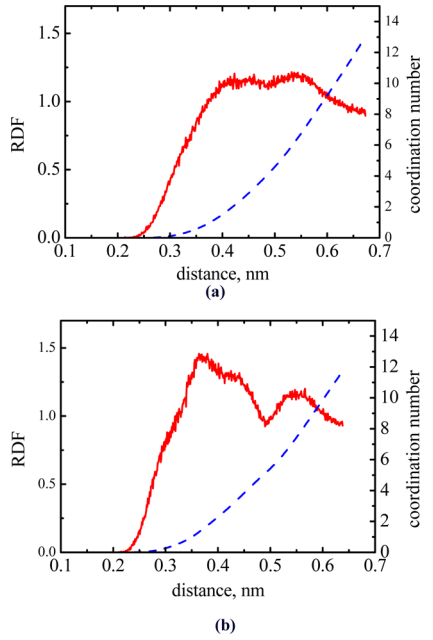

Figure 3. Coordination number (dashed line) plotted up to first minimum of the radial distribution function (solid line, left) calculated for $S_2O_8^{2-}$ (a) and $S_2O_8^{3-}$ (b) in ethylene glycol (x(EG) = 1).

Table 2. Coordination Numbers Corresponding to the Nearest Solvation Sheath of $S_2O_8^{2-}$ and $S_2O_8^{3-}$ in Water and EG Calculated from the Molecular Dynamics Simulations

	water		ethylene glycol	
	$S_2O_8^{2-}$	$S_2O_8^{3-}$	$S_2O_8^{2-}$	$S_2O_8^{3-}$
coordination number	25	26	13	12
distance of the first minimum of RDF (nm)	0.577	0.564	0.673	0.638

Table 3. Reorganization Energies (kcal mol^{-1}) of the Reduction (Oxidation) of a Peroxodisulphate Anion in Different Water–EG Mixtures[a]

x(EG)	$\vec{\lambda}_s$	$\overleftarrow{\lambda}_s$	λ_s (eq 19)
0	22.4 (15.8)	54.5 (60)	33.2 (27.5)
0.3	18.7 (17.1)	68 (32.3)	32.1 (22.9)
0.5	25.6	54.7	36.3
1.0	38.3	32.2	34.9

[a]Results obtained for T = 350 K are given in parentheses.

important and qualitatively interesting feature predicted on the basis of atomistic MD simulations. In a previous work[12] a very slight change of the solvent reorganization energy for the thermal electron transfer within a $Co(NH_3)_5(pz)^{3+}/Fe(CN)_6^{4-}$ ion pair in water–EG mixtures (x(EG) = 0.09 to 0.58) was assumed using the analysis of the Pekar factor. Note that the reduction of $S_2O_3^{2-}$ at a metal electrode is a heterogeneous electron transfer. To address the effect of a metal surface in terms of a continuum approach, one should correct the solvent reorganization energy by the image term:[41]

$$\lambda_s^* = \lambda_s - \frac{Ce_0^2}{4x} \tag{20}$$

where x is the distance from the reactant center to the image plane (which is shifted ~0.1 nm from the position of the first layer of metal atoms toward solution).

dx.doi.org/10.1021/jp405097c | J. Phys. Chem. B 2013, 117, 8793–8801

If we take a value of 0.4 nm as a reasonable estimate for x, the image term ranges from 9.5 (EG) to 11 kcal mol^{-1} (water) and reduces the λ_s values obtained from MD simulations. Note that quantum solvent modes do not contribute to the classical activation barrier and should be cut from the outer-sphere reorganization energy. This effect is normally addressed by a coefficient ξ (<1) reducing λ_s:[3]

$$\xi = \frac{2}{\pi C}\int_0^{\omega^*} \frac{\mathrm{Im}\,\varepsilon(\omega)}{\omega\,|\varepsilon(\omega)|^2}\,\mathrm{d}\omega \tag{21}$$

where $\varepsilon(\omega)$ is the complex dielectric spectrum of the medium and the boundary cyclic frequency ω^* roughly separates classic and quantum regions of solvent modes.

For pure water, the coefficient ξ was previously estimated to be 0.8[3]. It is difficult to make pertinent estimations for EG and its mixtures with water because the available dielectric spectra poorly describe the high-frequency region.[6] Nevertheless, corrections of λ_s for the pure water image term (x(EG) = 0, see Table 3) and for quantum modes yield a value of 17.8 kcal mol^{-1}, which is very close to an estimate of the environmental reorganization energy of the reduction of $S_2O_8^{2-}$ made in ref 1 on the basis of a continuum model.

We also tried to investigate the influence of temperature on the reorganization energy for pure water and a certain EG–water mixture. (See Table 3.) The increase in temperature leads to a significant decrease in λ_s for a pure aqueous solution; in the mixed solution at x(EG) = 0.3 the decrease in the reorganization energy is smaller. This temperature effect cannot be explained in terms of a temperature-dependent Pekar factor.[42−44] According to the results of molecular dynamics simulations reported in works[43,44] the solvent reorganization energy can be recast as a sum of two terms. The first term arises from the orientational structure factors, while the second contribution originates from solvent density fluctuations. The second term was found by the authors[43,44] and is basically responsible for the negative temperature dependence of the solvent reorganization energy.

All Brownian dynamics simulations were performed at room temperature; a value of 17.8 kcal mol^{-1} was taken for λ_s, which does nor depend on the EG content (see above). We observed that the reaction system moves slowly in "grooves" on the free-energy surface along the solvent coordinates permanently making fast attempts to overcome the saddle line along the intramolecular degree of freedom. The rate constants versus the EG content calculated at several electrode overvoltages are shown in Figure 4. It can be seen from Figure 4 that starting from η = 2.9 V the k versus x(EG) dependencies increase with increasing EG content. The ascending plots become more pronounced at higher overvoltages. Therefore, the results obtained are qualitatively in good agreement with the experimental data.[6] Another quantity that is useful to describe electrochemical redox systems is transfer coefficient α:

$$\alpha = -\frac{k_B T}{e_0}\frac{\partial \ln k}{\partial \eta} \tag{22}$$

The transfer coefficient α calculated as a function of x(EG) is shown in Figure 5; a linear approximation was used to fit the ln $k(\eta)$ dependencies. The α values are noticeably <0.5 which is typical for electron-transfer reactions proceeding in the vicinity of activationless discharge, that is, at large electrode overvoltages. The increase in α with the growth of EG content (solvent viscosity) agrees with the experimental findings previously reported[6] and the data obtained for water–glucose (sucrose) solutions.[7] Other examples of a nonmonotonous dependence of transfer coefficient on electrode overpotential calculated on the basis of Sumi–Marcus model as a function of solution viscosity are also presented in work.[45]

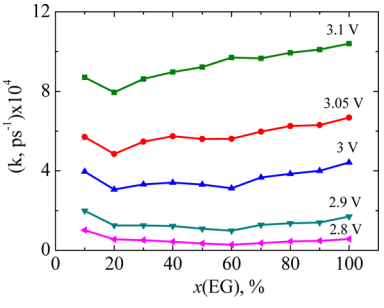

Figure 4. Rate constant of the $S_2O_8^{2-}$ reduction from content in water–EG mixtures versus EG calculated at different electrode overpotentials (2.8 to 3.1 V).

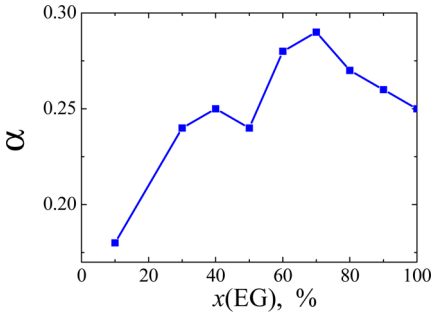

Figure 5. Symmetry coefficient describing the reduction of a peroxodisulphate anion at a mercury electrode from mixed water–EG solutions calculated as a function of x(EG).

We also calculated the Kramer's transmission coefficient (κ_{Kr}) (one should distinguish between the Kramer's transmission coefficient and electronic transmission coefficient; the latter is assumed to be nearly 1 in our case), which is a measure of the effect of solvent dynamics, or, in other words, of the deviation from simple transition state theory (TST):

$$\kappa_{Kr} = k/k_{TST} \tag{23}$$

where k is the rate constant calculated from the Brownian dynamics simulations and k_{TST} is calculated on the basis of TST.

The κ_{Kr} values were found to be noticeably <1 (see Figure 6), which points to the significant role of solvent dynamics effect.

The saddle point avoidance (SPA) is one of the most remarkable manifestations of solvent dynamics effects; the larger this effect is, the slower the reaction rate is. Because in our case the intramolecular coordinate is fast, it is reasonable to describe the SPA as a sum of contributions from all solvent modes:

$$\delta q_{solv} = \sum_{i=1}^{3} (q_i^* - q_i^{saddle}) \tag{24}$$

where q_i^* are the solvent modes corresponding to the reaction window and q_i^{saddle} are the solvent coordinates of the saddle point of 5D free-energy surface.

dx.doi.org/10.1021/jp405097c | J. Phys. Chem. B 2013, 117, 8793−8801

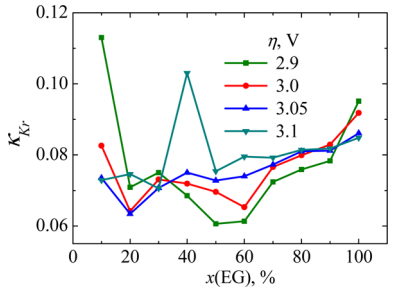

Figure 6. Kramer's transmission coefficient (κ_{Kr}) describing the $S_2O_8^{2-}$ reduction versus the EG content in water–EG mixtures calculated at different electrode overpotentials (η).

The dependence of δq_{solv} on x(EG) calculated at η = 3 V is plotted in Figure 7. As shown in our analysis, the

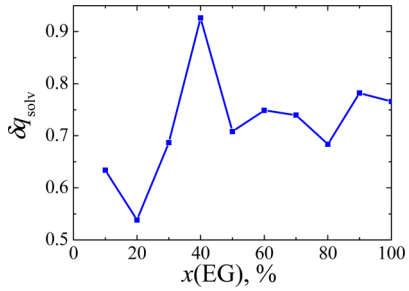

Figure 7. Saddle-point avoidance effect (see eq 23) as a function of the EG content presented at η = 3.1 V.

nonmonotonous behavior of the model k versus x(EG) curves can be explained in terms of the SPA; namely, this effect was found to be the largest at the vicinity of the $k(x(EG))$ minima.

In former works,[46−48] another version of Brownian dynamics (developed by Kast et al.[49]) was employed to address solvent dynamics effects in molecular dynamics simulations of electron-transfer reactions. In this method, friction effects are addressed by a bath of virtual particles with a Maxwell distribution of velocities that collide with the real particles. These authors[46−48] performed molecular dynamics simulations on 2D[46] and 3D[47,48] reaction free-energy surfaces to obtain the rate constants.

4. CONCLUDING REMARKS

With the help of molecular dynamics simulations we investigated the reduction of peroxodisulfate anion solvated in water–EG mixtures. The outer-sphere reorganization energy of electron transfer at the reduction of $S_2O_8^{2-}$ from mixed solutions was calculated in a simplified way. The averaged reorganization energy increases slightly with increasing EG fraction in the mixed solutions. This means that the static solvent effect does not contribute to the presence of a minimum in the experimental current versus solvent viscosity curves describing the electroreduction of a peroxodisulphate anion in these solvents.[6] This effect must, therefore, result from intrinsic dynamical properties of the key solvent modes that contribute to the observed electron-transfer rate. Our numerical results resting on the Brownian dynamics simulations with a nearly constant λ_s performed on a 5D reaction free-energy surface confirm this conclusion. The characteristic times of these modes and their contributions to the reaction free-energy surface can be extracted from the analysis of solvent correlation function. Each mode can be attributed to some special motion of EG and water molecules (rotation, the change of torsion angles, the lifetime of intra- or intermolecular H bond, etc). Such a "multi-mode" treatment of solvent dynamics in the Zusman's sense[4,16,52] seems to be crucial, because our calculations performed in the framework of the "one-mode" Sumi–Marcus model (with a constant λ_s) fail to describe the experimental effect even in a wide interval of the solution viscosity values (see Figure 2S in Supporting Information, Section A3). One may state that various solvent modes in electron-transfer reactions do not behave chaotically; their interplay resembles somewhat an orchestra where each solvent mode plays the role of one instrument. To judge, however, about the extent of generality of this finding, one needs first of all to investigate systematically solvent dynamics effects in pure "non-Debye" solvents (like glycerol, for example) from both experimental and theoretical viewpoints. The most remarkable manifestation of such an effect might be expected for interfacial electron transfer reactions occurring in the vicinity of activationless discharge because in this case large electrode overpotentials result in a significant decreasing the activation barrier. Thus, for a homogeneous redox process in water–EG mixtures the authors of ref 12 observed only a slight decreasing of the rate constant with the growth of EG content. The significant asymmetry of solvent reorganization is another conspicuous feature that deserves explanation at a microscopic level. A deeper insight into this feature can be gained from the analysis of the power spectra (the Fourier transform of the velocity autocorrelation function) describing the solvation shell of a peroxodisulphate anion in oxidized and reduced states.

■ ASSOCIATED CONTENT

Supporting Information

Partial charges and van der Waals potential parameters used in the MD simulations (Section A1, Table 1S). A graphic illustrating the calculation (according to eq 15) of free-energy surfaces for the electron transfer reaction $S_2O_8^{2-} + e = S_2O_8^{3-}$ in a water–EG mixture, x(EG)=0.5 (Section A2, Figure 1S). Results obtained in the framework of Sumi–Marcus model and some pertinent details of the calculations (Section A3, Figure 2S). The full list of authors in refs 24 and 50 (Section A4). This material is available free of charge via the Internet at http://pubs.acs.org.

■ AUTHOR INFORMATION

Notes

The authors declare no competing financial interest.

■ ACKNOWLEDGMENTS

This work was partially supported by the RFBR (project no. 11-03-01186-a) and by the project I200-N19 of the Austrian Science Fund FWF. We are deeply indebted to Galina Tsirlina and Pavel Zagrebin for very useful and stimulating discussions. We also thank Michael Bronshtein and Tamara Zinkicheva for the help with calculations.

■ REFERENCES

(1) Nazmutdinov, R. R.; Glukhov, D. V.; Tsirlina, G. A.; Petrii, O. A. Molecular Description of the Persulfate Ion Reduction on a Mercury Electrode. *Russ. J. Electrochem.* **2002**, *38*, 720–731.

(2) Nazmutdinov, R. R.; Glukhov, D. V.; Petrii, O. A.; Tsirlina, G. A.; Botukhova, G. N. Contemporary Understanding of the Peroxodisulfate

Reduction at a Mercury Electrode. *J. Electroanal. Chem.* **2003**, *552*, 261−278.
(3) Kuznetsov, A. M. *Charge Transfer in Physics, Chemistry and Biology: The Physical Mechanism of Elementary Processes and Introduction to the theory*; Gordon and Breach: Berkshire, U.K., 1995.
(4) Kuznetsov, A. M. *Stochastic and Dynamic Views of Chemical Reaction Kinetics in Solutions*. Presses Polytechniques et Universitaires Romandes: Lausanne, 1999.
(5) Titova, N. V.; Laurinavichute, V. K.; Kuz'minova, Z. V.; Tsirlina, G. A. Electroreduction of Peroxodisulfate on Mercury in Mixed Water-Carbohydrate Media: The Interplay of Solvent Effects and Concentration-Dependent Structure of Reaction Layer. *Chem. Phys.* **2008**, *352*, 345−352.
(6) Zagrebin, P. A.; Buchner, R.; Nazmutdinov, R. R.; Tsirlina, G. A. Dynamic Solvent Effects in Electrochemical Kinetics: Indications for a Switch of the Relevant Solvent Mode. *J. Phys. Chem B.* **2010**, *114*, 311−320.
(7) Nazmutdinov, R. R.; Bronshtein, M. D.; Tsirlina, G. A.; Titova, N. V. Interplay Between Solvent Effects of Different Nature in Interfacial Bond Breaking Electron Transfer. *J. Phys. Chem B.* **2009**, *113*, 10277−10284.
(8) Sumi, H.; Marcus, R. A. Dynamical Effects in Electron Transfer Reactions. *J. Chem. Phys.* **1986**, *84*, 4894−4914.
(9) Morillo, M.; Denk, C.; Pérez, P.; López, M.; Sánchez, A.; Prado, R.; Sánchez, F. Electron Transfer Reactions in Solvent Mixtures: the Excess Component of Solvent Reorganization Free Energy. *Coord. Chem. Rev.* **2000**, *204*, 173−198.
(10) Pérez, F.; Hermández, R.; Prado-Gotor, R.; Lopes-Costa, T.; López-Cornejo, P. Method for the Evaluation of the Reorganization Energy of Electron Transfer Reactions in Water Methanol Mixtures. *Chem. Phys. Lett.* **2005**, *407*, 342−346.
(11) Denk, C.; Morillo, M.; Sánchez-Burgos, F.; Sánchez, A. Reorganization Energies for Charge Transfer Reactions in Binary Mixtures of Dipolar Hard Sphere Solvents: A Monte Carlo Study. *J. Chem. Phys.* **1999**, *110*, 473−483.
(12) Sánchez, F.; Rodríguez, A.; Muriel, F.; Burgess, J.; López-Cornejo, P. Kinetic Study of the Electron Transfer Process Between $Ru(NH_3)_5pz^{2+}$ and $S_2O_8^{2-}$ in Water−Cosolvent Mixtures: a New Component of Reorganization Energy. *Chem. Phys.* **1999**, *243*, 159−168.
(13) Muriel, F.; Jiménez, R.; López, M.; Prado-Gotor, R.; Sánchez, F. Solvent Effects on the Oxidation (Electron Transfer) Reaction of $[Fe(CN)_6]^{4-}$ by $[Co(NH_3)_5pz]^{3+}$. *Chem. Phys.* **2004**, *298*, 317−325.
(14) Sparpaglione, M.; Mukamel, S. Dielectric Friction and the Transfer from Adiabatic to Nonadiabatic Electron Transfer in Condensed Phases. II. Application to Non-Debye Solvents. *J. Chem. Phys.* **1986**, *88*, 4300−4311.
(15) Zusman, L. D. Electron Transfer Reactions at an Electrode in Solvents with Two Characteristic Relaxation Times. *Soviet Electrochem.* **1989**, *24*, 1125−1132.
(16) Zusman, L. D. The Theory of Electron Transfer Reactions in Solvents with Two Characteristic Relaxation Times. *Chem. Phys.* **1988**, *119*, 51−61.
(17) Basilevsky, M. V.; Chudinov, G. E. Kinetics of Outer-Sphere Electron Transfer in Non-Debye Solvents With Two Characteristic Relaxation Times. *Mol. Phys.* **1990**, *71*, 461−476.
(18) Allen, M. P.; Tildesley, D. J. *Computer Simulation of Liquids*; Clarendon Press: Oxford, 1987.
(19) Rose, D. A.; Benjamin, I. Molecular Dynamics of Adiabatic and Nonadiabatic Electron Transfer at the Metal-Water Interface. *J. Chem. Phys.* **1994**, *100*, 3545−3555.
(20) Small, D. W.; Matyushov, D. V.; Voth, G. A. The Theory of Electron Transfer Reactions: What May be Missing? *J. Am. Chem. Soc.* **2003**, *125*, 7470−7478.
(21) Matyushov, D. V. Standard Electrode Potential, Tafel Equation and the Solvation Thermodynamics. *J. Chem. Phys.* **2009**, *130*, 234704−234714.
(22) Martin, D. R.; Matyushov, D. V. Non-Gaussian Statistics and Nanosecond Dynamics of Electrostatic Fluctuations Affecting Optical Transitions in Proteins. *J. Phys. Chem. B.* **2012**, *116*, 10294−10300.
(23) Cornell, W. D.; Cielak, P.; Bayly, C. I; Kollman, P. A. Application of RESP charges to calculate conformational energies, hydrogen bond energies, and free energies of solvation. *J. Am. Chem. Soc.* **1993**, *115*, 9620.
(24) Case, D. A.; Darden, T. A.; Cheatham, T. E., III; Simmerling, C. L.; Wang, J.; Duke, R. E.; Luo, R.; Walker, R. C.; Zhang, W.; Merz, K. M.; et al. *AMBER 12*: University of California: San Francisco, 2012.
(25) Berendsen, H. J. C.; Grigera, J. R.; Straatsma, T. P. The Missing Term in Effective Pair Potentials. *J. Phys. Chem.* **1987**, *91*, 6269−6271.
(26) Tombari, E.; Presto, S.; Salvetti, G. Heat Capacity of Tetrahydrofuran Clathrate Hydrate and of its Components, and the Clathrate Formation from Supercooled Melt. *J. Chem. Phys.* **2006**, *124*, 154507−154516.
(27) Gubskaya, A. V.; Kusalik, P. G. Molecular Dynamics Simulation Study of Ethylene Glycol, Ethylenediamine, and 2-Aminoethanol. 2. Structure in Aqueous Solutions. *J. Phys. Chem. A.* **2004**, *108*, 7151−7178.
(28) Jorgensen, W. L.; Tirado-Rives, J. The OPLS [Optimized Potentials for Liquid Simulations] Potential Functions for Proteins, Energy Minimizations for Crystals of Cyclic Peptides and Crambin. *J. Am. Chem. Soc.* **1988**, *110*, 1657−1666.
(29) Allinger, N. L.; Yuh, Y. H.; Lii, J.-H. Molecular Mechanics. The MM3 Force Field for Hydrocarbons. 1. *J. Am. Chem. Soc.* **1989**, *111*, 8551−8566.
(30) Kumbharkhane, A. C.; Puranik, S. M.; Mehrotra, S. C. Temperature Dependent Dielectric Relaxation Study of Ethylene Glycol-Water Mixtures. *J. Solution Chem.* **1992**, *21*, 201−212.
(31) Hummer, G.; Pratt, L. R.; Garcia, A. E. Free Energy of Ionic Hydration. *J. Phys. Chem.* **1996**, *100*, 1206−1215.
(32) Ben-Naim, A.; Markus, Y. Solvation Thermodynamics of Nonionic Solutes. *J. Chem. Phys.* **1984**, *81*, 2016−2027.
(33) Hawkins, G. D.; Gramer, S. J.; Truhlar, D. G. Universal Quantum Mechanical Model for Solvation Free Energies Based on Gas-Phase Geometries. *J. Phys. Chem. B* **1998**, *102*, 3257−3271.
(34) Hummer, G.; Pratt, L. R.; Garcia, A. E; Berne, B. J.; Rick, S. W. Electrostatic Potentials and Free Energies of Solvation of Polar and Charged Molecules. *J. Phys. Chem. B.* **1997**, *101*, 3017−3020.
(35) Warren, G. L.; Patel, S. Hydration Free Energies of Monovalent Ions in Transferable Intermolecular Potential Four Point Fluctuating Charge Water: An Assessment of Simulation Methodology and Force Field Performance and Transferability. *J. Chem. Phys.* **2009**, *127*, 064509−064527.
(36) Horinek, D.; Mamatkulov, Sh. I.; Netz, R. R. Rational Design of Ion Force Fields Based on Thermodynamic Solvation Properties. *J. Chem. Phys.* **2009**, *130*, 124507−124527.
(37) Mamatkulov, Sh. I.; Ismailova, O. B.; Ashirmatov, S. The Influence of Pressure on the Stability of Clathrate Hydrates of Hydrogen and Tetrahydrofuran. *Russ. J. Phys. Chem. A* **2011**, *85*, 760−766.
(38) Hess, B.; Kutzner, C.; van der Spoel, D.; Lindahl, E. GROMACS 4: Algorithms for Highly Efficient, Load-Balanced, and Scalable Molecular Simulation. *J. Chem. Theory Comput.* **2008**, *4*, 435−447.
(39) Nazmutdinov, R. R. Quantum Chemical Description of Charge Transfer Processes at the Metal/Solution Interface: Yesterday, Today and Tomorrow. *Russ. J. Electrochem.* **2002**, *38*, 111−122.
(40) Curtiss, L. A.; Halley, J. W.; Hautman, J.; Hung, N. C.; Nagy, Z.; Rhee, Y.-J.; Yonco, R..M. Temperature Dependence of the Heterogeneous Ferrous-Ferric Electron Transfer Reaction Rate: Comparison of Experiment and Theory. *J. Electrochem. Soc.* **1991**, *138*, 2032−2040.
(41) Marcus, R. A. On the Theory of Electron-Transfer Reactions. VI. Unified Treatment for Homogeneous and Electrode Reactions. *J. Chem. Phys.* **1965**, *43*, 679−701.
(42) Leontyev, I. V.; Tovmash, A. V.; Vener, M. V.; Rostov, I. V.; Basilevsky, M. V. Molecular Simulations of Outersphere Reorganiza-

tion Energies for Intramolecular Electron and Hole Transfer in Polar Solvents. *Chem. Phys.* **2005**, *319*, 4−15.
(43) Vath, P.; Zimmt, M. B.; Matyushov, D. V.; Voth, G. A. A Failure of Continuum Theory: Temperature Dependence of Solvent Reorganization Energy of Electron Transfer in Highly Polar Solvents. *J. Phys. Chem.* **1999**, *103*, 9130−9140.
(44) Ghorai, P. K.; Matyushov, D. V. Solvent Reorganization Entropy of Electron Transfer in Polar Solvents. *J. Phys. Chem.* **2006**, *110*, 8857−8863.
(45) Petrii, O. A.; Nazmutdinov, R. R.; Bronshtein, M. D.; Tsirlina, G. A. Life of the Tafel Equation: Current Understanding and Prospects for the Second Century. *Electrochim. Acta* **2007**, *52*, 3493−3504.
(46) Kuznetsov, A. M.; Schmickler, W. A Simulation of an Electrochemical Adiabatic Electron- Transfer Reaction. *Chem. Phys. Lett.* **2000**, *327*, 314−318.
(47) Ignaczak, A.; Schmickler, W. Simulations of Adiabatic Bond-Breaking Electron Transfer Reactions on Metal Electrodes. *Chem. Phys.* **2002**, *278*, 147−158.
(48) Ignaczak, A. Comparison of Temperature Effect on Electroreduction of Tert-Butyl Chlorides and Tert-Butyl Bromides − Theoretical Studies. *Electrochim. Acta* **2011**, *56*, 6305−6311.
(49) Kast, S. M.; Nicklas, K.; Bär, H.-J.; Brickman, J. Constant Temperature Molecular Dynamics Simulations by means of a Stochastic Collision Model. I. Non-Interacting Particles. *J. Chem. Phys.* **1994**, *100*, 567−576.
(50) Frisch, M. J.; Trucks, G. W.; Schlegel, H. B.; Scuseria, G. E.; Robb, M. A.; Cheeseman, J. R.; Scalmani, G.; Barone, V.; Mennucci, B.; Petersson, G. A.; et al. *Gaussian 09*, revision A.1; Gaussian, Inc.: Wallingford, CT, 2009.
(51) Tsirlina, G. A.; Kharkats, Yu.I.; Nazmutdinov, R. R.; Petrii, O. A. Asymmetry of Inner-Sphere Reorganization Energy for Heterogeneous Electron Transfer. *J. Electroanal. Chem.* **1998**, *450*, 63−68.
(52) Zusman, L. Outer-Sphere Electron Transfer in Polar Solvents. *Chem. Phys.* **1980**, *49*, 295−304.